Predissociation Mechanism and Dynamics of HCP†

Masahito Namai, Toshiyuki Sasaki, Haruki Ishikawa,*,‡ Hiromi Morikuni, and Naohiko Mikami

Department of Chemistry, Graduate School of Science, Tohoku University, Aoba-ku, Sendai 980-8578, Japan

Received: January 15, 2009; Revised Manuscript Received: March 11, 2009

In the present study, we have observed absorption, fluorescence excitation, and CP radical action spectra of the HCP molecule in the vicinity of the dissociation threshold to $H(^2S) + CP(X\ ^2\Sigma^+)$. In addition, we have measured the rotational distribution of the CP radical produced from certain single rovibronic levels of the parent HCP molecule. It is found that the CP radical action spectrum starts to appear at the point where the fluorescence intensity decreases suddenly. On the basis of the precise energetic consideration between the parent and the product rovibronic energies, the dissociation energy of HCP to $H(^2S) + CP(X\ ^2\Sigma^+)$ is determined to be 41 662.3 ± 0.5 cm^{-1}. The energy distribution in the predissociation is found to be basically statistical; however, the prominent preferences in the rotational distributions or nonstatistical distributions are observed only when the vibronic energy of the parent level is smaller than the dissociation threshold energy. This preference is qualitatively interpreted by the inefficient energy transfer from the rotational to the vibrational degrees of freedom in the exit region of the $\tilde{X}$ state potential energy surface. As a result, the dissociation proceeds along the linear H−C−P configuration, and this geometrical restriction makes nonstatistical rotational distribution of the CP radical.

1. Introduction

HCP is a phosphorus analogue of HCN. In the past decade, vibrational dynamics in highly excited vibrational levels of the electronic ground, $^1\Sigma^+$, state of HCP was extensively studied both experimentally and theoretically with respect to the isomerization from HCP to CPH.[1−23] In contrast, the number of studies on the excited electronic state of HCP is much smaller than that on the $\tilde{X}$ state. The first and extensive observation of electronic transitions of HCP was carried out by Johns and co-workers.[24] They observed a large number of electronic absorption bands and assigned three singlet ($\tilde{A}\ ^1A''$, $\tilde{B}\ ^1\Pi$, and $\tilde{C}\ ^1A'$) and four triplet ($\tilde{a}\ ^3\Sigma^+$, $\tilde{b}\ ^3\Pi$, $\tilde{c}\ ^3\Sigma^-$, and $\tilde{d}\ ^3\Pi$) excited states. Later, the $\tilde{B}$ state was reassigned to be a mixed state between the $\tilde{A}$ and a $^3\Delta$ state by both experimental and theoretical studies.[25,26] In 1993, Mason and Lehmann observed fluorescence excitation (FE) spectra of HCP in a jet-cooled condition.[27,28] They carried out Fourier transformation of fluorescence decay profiles and confirmed that the perturber of the $\tilde{B}$ state is a $^3\Delta$ state. In addition, they found a sharp decrease in fluorescence intensity in the LIF spectra at 41 680 cm^{-1}. They attributed it to a dissociation of HCP to $H(^2S) + CP(X\ ^2\Sigma^+)$. However, the CP radicals produced in the dissociation were not observed in their study. Electronic excited states in a much higher energy region have been observed by optical−optical double resonance spectroscopy. On the basis of the selection rules of observed transitions, 2 $^1A''$[29] and 3 $^1A'$[30,31] states have been identified.

So far, a number of theoretical studies on the excited electronic states have been carried out.[26,32−35] Essentially, it was expected that potential energy surfaces of both the $\tilde{A}$ and the $\tilde{C}$ states are very shallow along the bending coordinate and that there are several local minima in each potential energy surface. Nanbu and co-workers carried out high-level theoretical calculations of the excited electronic state of HCP.[34] They obtained potential energy surfaces of the $\tilde{X}\ ^1\Sigma^+$, $\tilde{A}\ ^1A''$, $\tilde{C}\ ^1A'$, and 2 $^1A''$ states. The bending potential curves of these states obtained by them essentially coincided with former results of theoretical calculations. In addition to the calculation of the potential energy surfaces, they obtained energies and wave functions of several vibrational levels in these electronic states. They also suggested that there is a nonadiabatic interaction between the $\tilde{C}$ and the $\tilde{X}$ states along the bending coordinate. This interaction is expected to be one of the origins of the predissociation. Very recently, Ingels and co-workers have carried out a high level ab initio calculation on singlet ground and low-lying electronic excited states of HCP and also HPC.[35] They have derived the dissociation energy of the $\tilde{X}$ state to $H(^2S) + CP(X\ ^2\Sigma^+)$ to be 119.0 kcal mol^{-1} (41650 cm^{-1}). This value well reproduced the dissociation energy reported by Mason and Lehmann.[27,28]

The photodissociation dynamics of small molecules has been thoroughly investigated by many researchers. However, it is a very fundamental and a very important process in the photophysical and chemical processes.[36−40] We have been carrying out spectroscopic studies on HCP in both the ground and excited electronic states.[5−8,41] In the course of our study, it has been found that several vibronic bands appear in FE spectra in the energy region above the dissociation threshold (41 680 cm^{-1}) reported by Mason and Lehmann.[27,28] Thus, the dissociation threshold of HCP has been re-examined in the present study. In addition, to reveal the mechanism and dynamics of the predissociation of HCP, several kinds of experiments have been carried out. In the present study, we have succeeded in observing the product CP radical as direct evidence of the dissociation. CP action, FE, and also absorption spectra have been measured and compared to discuss the mechanism and dynamics of the predissociation of HCP. In addition to these spectroscopic measurements, many sets of rotational distribution of the CP radicals produced from a single rovibronic level of HCP were

† Part of the "Robert W. Field Festschrift".

* To whom correspondence should be addressed. Fax: +81-78-803-6463. E-mail: haruki@kobe-u.ac.jp.

‡ Present address: Department of Chemistry, Graduate School of Science, Kobe University, Nada-ku, Kobe 657-8501, Japan.

10.1021/jp900450t CCC: $40.75
Published on Web 04/09/2009

measured by laser-induced fluorescence (LIF) method. This measurement is a so-called 'state-to-state' observation of the chemical reaction, and it should provide us with important information about the reaction dynamics. In the present paper, we report the precise determination of the dissociation energy of HCP to $H(^2S) + CP(X\ ^2\Sigma^+)$, then we discuss the mechanism and dynamics of the predissociaiton of the HCP molecule in the electronic excited $\tilde{A}$ and $\tilde{C}$ states in the very vicinity of the dissociation threshold.

2. Experimental Details

HCP was synthesized by either a pyrolysis of CH_3PCl_2[3] or a vacuum gas−solid HCl elimination reaction method of $CHCl_2$-PH_2.[27,28] As reported by Mason, the latter method provides the HCP molecule with fewer impurities.[28] To avoid the decomposition of the HCP molecule, all sample bottles, vacuum lines, and fluorescence measurement cells made of glass were used. HCP was stored at the liquid N_2 temperature. By heating the sample bottle to gain the vapor pressure, HCP was introduced into the fluorescence measurement cell. The sample gas was not flowed during the measurements below but stored in the cell for several hours. Since relative populations among the dissociation products were important in the present study, the crude pressure of HCP was sufficient to perform the experiment. Thus, we used a general pirani gauge to measure the total pressure of the sample gas, which was set just in front of the sample inlet to the cell. To minimize the contact of HCP to the metal part of the pressure gauge, the total pressure was measured only when the sample was being introduced into the cell. The total pressure of the sample was about 300 mTorr. In the case of absorption spectroscopy, it was raised to 1 or 2 Torr to gain a strong enough signal.

The experimental apparatus used in the present study is basically the same as that described elsewhere.[6] A frequency-doubled output of a tunable dye laser (Lambda Physik SCANmate 2E) pumped by a Nd:YAG laser (Continuum Powerlite 9010) was introduced into the fluorescence measurement cell. This laser light was used to excite the HCP molecules to their electronic excited states. Fluorescence from the electronic excited state of HCP was collected by a lens system onto a photomultiplier tube (PMT) (Hamamatsu R1527) at a right angle to the laser beam. A small portion of the laser output is used to measure the sorption spectra of $^{130}Te_2$. The wavenumber was calibrated against the $^{130}Te_2$ atlas.[42]

CP radicals generated by the pump laser light were detected by LIF spectroscopy. A frequency-doubled output of another Nd:YAG laser pumped dye laser was tuned to the $B\ ^2\Sigma^+ - X\ ^2\Sigma^+$ transition of the CP radical. The probe laser beam was introduced into the cell from the direction opposite that of the pump laser beam. When LIF spectra of the CP were measured, a 25 cm monochromator was set in front of the PMT to avoid intense fluorescence from the parent HCP molecule. A typical delay time between the pump and the probe pulses was 20 ns. We confirmed that there is no substantial rotational relaxation of the product CP in our experimental condition by changing the delay time and sample pressure. The probe laser wavenumber was calibrated using the reported molecular constants of the CP radical.[43]

In the case of the pump−probe measurements, to reduce an effect of the shot-to-shot fluctuation of the pump laser intensity, the pump laser pulse was divided into two portions by a beamsplitter and then introduced into the fluorescence signal cell as well as a reference fluorescence cell that is identical to the fluorescence signal cell. These cells were connected by the tube to keep the sample condition the same. The total fluorescence intensity of HCP was measured in the reference cell. The probe laser pulse was introduced only into the signal cell. The reference signal was used for the reduction of the effect of the fluctuation of the pump pulse intensity. As mentioned above, the measurements were carried out in static conditions. Thus, the parent HCP molecule decreases with time. This long time change in the HCP amount was also corrected by the reference signal intensity.

In the case of absorption spectroscopy, we used an absorption cell 1 m long, and the laser path length was set to 2 m. Partial laser beam intensity before entering the absorption cell was monitored and used for the correction of the intensity fluctuation of the pump laser pulse.

To avoid confusion, the term of "fluorescence excitation (FE)" is used in the present paper for the excitation of the parent HCP molecule, whereas the term "laser-induced fluorescence (LIF)" is used for the product CP radical.

3. Results and Discussion

3.1. Observation of the Electronic Excited-State of HCP above the Dissociation Threshold. Mason and Lehmann measured FE spectra of jet-cooled HCP and found a sharp decrease in fluorescence intensity at 41 680 cm^{-1} and attributed it to the dissociation of HCP into $H(^2S) + CP(X\ ^2\Sigma^+)$.[27,28] Above this energy region, any vibronic levels were observed in their study. In the present study, we have measured FE spectra of HCP in this energy region under room temperature conditions. The FE spectrum in the vicinity of the dissociation limit of HCP obtained in the present study is shown in the middle trace of Figure 1. As clearly seen in the figure, a sharp decrease in intensity has been observed at 41 680 cm^{-1}. This behavior is consistent with the observation by Mason and Lehmann.[27,28] To confirm that this decrease in the LIF intensity originates from the sudden onset of a nonradiative process, we have also recorded the absorption spectrum in the same energy region. In contrast to the FE spectrum, there is no decrease in intensity in the absorption spectrum in the energy region covered in the figure, as shown in the top trace in Figure 1. This observation indicates that some nonradiative processes start to occur at this energy region. As pointed out by Mason and Lehmann, the most probable process is predissociation of HCP. The direct evidence of the predissociation is to observe product CP radicals. To detect the product CP radical, the $B\ ^2\Sigma^+ - X\ ^2\Sigma^+$ transition of CP radicals was observed by the LIF method. Figure 2a shows a typical example of LIF spectrum of the CP radicals produced by the predissociation of the HCP molecule. Under our experimental conditions, splitting due to the spin−rotation interaction is not resolved in the LIF spectrum. The bottom trace in Figure 1 is an action spectrum recorded by monitoring LIF intensity of the R-head of the $B\ ^2\Sigma^+ - X\ ^2\Sigma^+$ (0−0) band of CP. The rovibronic transitions of HCP in the action spectrum start to appear at the very point where the intensity of the fluorescence shows the sharp decrease. A precise determination of the dissociation energy will be discussed later.

Figure 3 shows action spectra of HCP monitoring the product CP radical in a higher energy region than that shown in Figure 1. Note that rotationally resolved vibronic bands of HCP appear up to the 44 000 cm^{-1} energy region. In addition, no broadening of the rotational line width is observed. The line width is within the laserline width of ~0.2 cm^{-1}. This indicates that the lifetime of the upper state is on the order of subpicoseconds to nanoseconds and that there is no direct dissociation path up to this energy region. A monotonic decrease in intensity is probably

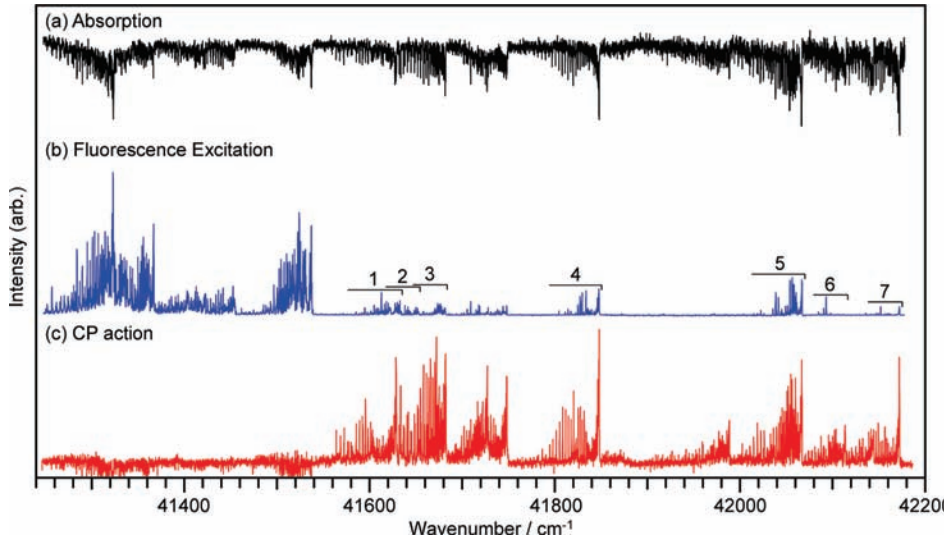

Figure 1. (a) Absorption, (b) fluorescence excitation, and (c) CP action spectra of HCP in the vicinity of the dissociation threshold. The CP action spectrum was recorded by probing the R-head of the B $^2\Sigma^+-$X $^2\Sigma^+$ (0−0) band. The vibronic bands used as the pump transitions in the present study are labeled as bands 1−7, as indicated in the figure.

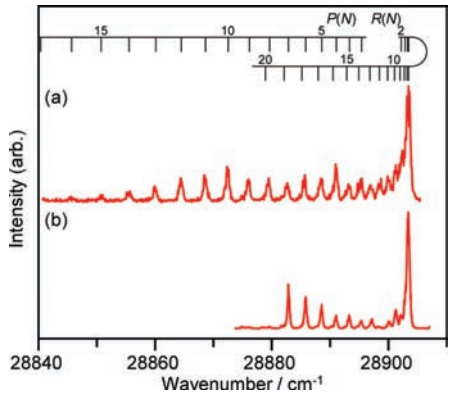

Figure 2. Laser-induced fluorescence (LIF) spectra of the B $^2\Sigma^+-$X $^2\Sigma^+$ (0−0) band of the CP radical produced in the predissociation of the HCP molecule. (a) Typical LIF spectrum obtained when the available energy in the dissociation is large. (b) LIF spectrum recorded when the $Q(7)$ line of band 3 was used as the pump transition.

due to a decrease in the Franck−Condon overlap between the ground and electronically excited states. The upper trace in Figure 3 is an action spectrum obtained by monitoring the vibrationally excited CP radical ($v = 1$). The difference in the appearance energies between the $v = 1$ and $v = 0$ CP radicals is about 1200 cm^{-1}, which corresponds to the vibrational energy of the CP radical (1232.8 cm^{-1}).[43]

The theoretical studies reported that the potential surface of both of the $\tilde{A}\ ^1A''$ and the $\tilde{C}\ ^1A'$ states have rather shallow minima along the bending angle.[26,32−35] Thus, assignments of the vibrational levels using vibrational quantum numbers such as (v_1, v_2, v_3) are difficult in the energy region where the predissociation occurs. To label vibrational levels or vibronic bands, hereafter, each vibronic band will be referred to as "band x", where $x = 1-7$, as indicated in Figure 1. Precise rotational analysis of these vibronic bands was not completed because of a lot of rotational perturbations. Severe rotational perturbations are found in the vibronic band between bands 3 and 4. Thus, this band is not referred to in the following discussion. Vibronic origins and rotational constants of the upper level of each band are summarized in Table 1.

3.2. Determination of the Dissociation Energy. In the present study, we observed many sets of rotational distribution of the product CP radical generated from single rovibronic levels of the parent HCP molecule. The LIF spectrum of the CP radical shown in Figure 2b is measured using the $Q(7)$ rotational line of band 3 as the pump transition. As can be seen, there is an upper limit of the rotational level of the CP radical produced. This limitation will be used in determining the dissociation energy, D_0. Since the single rovibronic level was selected as an initial state by the pump transition, the total or initial energy, E_{total}, was defined in each measurement. In the energy region just above the dissociation threshold, the available energy, E_{avl}, in the dissociation is distributed to the relative translational energy, E_{tr}, and the rotational energy of the CP radical, $E_{rot}^{CP}(N)$ since E_{avl} is not large enough to excite CP vibration. That is,

$$E_{avl} = E_{total} - D_0 = E_{tr} + E_{rot}^{CP}(N) \quad (1)$$

where N is a rotational quantum number of the CP radical in the Hund's case (b). Equation 1 can be rewritten as

$$E_{total} - E_{rot}^{CP}(N) = D_0 + E_{tr} \quad (2)$$

As shown in Figure 2b, the upper limit of the rotational level of the CP radical produced has clearly been observed. Here, the largest rotational quantum number of the CP radical observed is denoted as N_{max}. Since the value of E_{tr} must be ≥ 0, the value of D_0 can be estimated as

$$E_{total} - E_{rot}^{CP}(N_{max}) \geq D_0 \geq E_{total} - E_{rot}^{CP}(N_{max} + 1) \quad (3)$$

Here, an effect of the centrifugal barrier is neglected.[44] When $Q(8)$ rotational line of band 3 was used as the pump transition, the value of N_{max} was 8. In this case, the lower and upper limits of D_0 are obtained to be 41 648.48 and 41 662.80 cm^{-1}, respectively. Although the $Q(12)$ line of band 3 was used as the pump transition, the value of N_{max} is 10, and the lower and upper limits of D_0 are 41 661.90 and 41 679.40 cm^{-1}, respectively. Using these values, we can estimate that the value of D_0 is between 41 661.90 and 41 662.80 cm^{-1}. We have examined many sets of measurements and determined the value of D_0 to be 41 662.3 ± 0.5 cm^{-1}. The band 3 used here is a band perpendicular to the $\tilde{A}\ ^1A''$ state. When a parallel band, such as band 1 or 2, was used as the pump transition, the same value of D_0 was obtained.

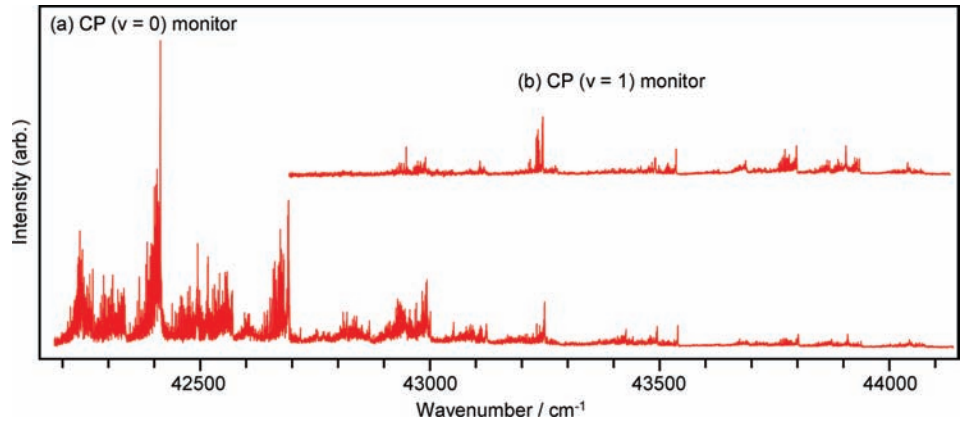

Figure 3. CP action spectra in the higher energy region than the dissociation threshold. (a) $v = 0$ and (b) $v = 1$ levels of the CP radical are monitored.

TABLE 1: Vibronic Origins, ν_0, and Rotational Constants of the Upper State, B, in the Bands of HCP Used in the Excitation in the Present Study and Symmetry of the Upper Electronic State

band[a]	ν_0/cm^{-1}	B/cm^{-1}	symmetry
1	41 624.1	0.603	A'
2	41 628.2	0.615	A'
2′	41 647.8	0.613	A'
3(e)[b]	41 679.8	0.573	A''
3(f)[b]	41 679.9	0.558	A''
4	41 843.6	0.602	A'
5(e)[b]	42 063.8	0.589	A''
5(f)[b]	42 064.0	0.604	A''
6(f)[c]	42 111.5	0.562	A''
7	42 167.7	0.602	A'

[a] Definition of the band numbering is shown in Figure 1. [b] The e- and f-symmetry components are analyzed separately. [c] Only the f-symmetry components are analyzed.

3.3. Predissociation Mechanism. As reported by Nanbu and co-workers, both $\tilde{A}$ and the $\tilde{C}$ states do not directly correlate to the H(^{2}S) + CP(X $^2\Sigma^+$) dissociation limit.[34] Thus, a nonadiabatic process from the initially excited electronic state to the $\tilde{X}$ state must occur during the dissociation. Rotational quantum number dependence of the relative yield of CP production should provide us with a clue to reveal the mechanism of the predissociation of HCP. To obtain the relative CP production yield, rotational line intensities in the CP action spectrum are normalized by those in the absorption spectrum. In addition, relative fluorescence yields were also estimated. The CP production yield in bands 1−3 severely depend on whether the total energy is higher than D_0. To avoid such an energetic restriction, bands whose vibronic energy is high enough with respect to D_0 are examined here.

Figure 4 exhibits absorption, FE, and CP action spectra of HCP of band 5. Band 5 is a perpendicular transition to the $\tilde{A}$ $^1A''$ state and the value of K'_a is 1. The FE spectrum of band 5 exhibits an irregular intensity pattern, especially in the P-branch. For instance, an intensity of P(9) rotational is much weaker than that of the neighboring P(10) line. In addition, the P(13) and P(14) lines do not appear in the FE spectrum. In contrast, the rotational line pattern of the absorption and the CP action spectra are almost regular and similar to each other. Relative fluorescence and CP production yields are plotted against $J(J + 1)$, as shown in Figure 5, together with a termvalue plot. Since the rotational energy is proportional to $J(J + 1)$ neglecting the centrifugal distortion term, the termvalue plot exhibits a smooth, straight line when there is no local perturbation. To emphasize

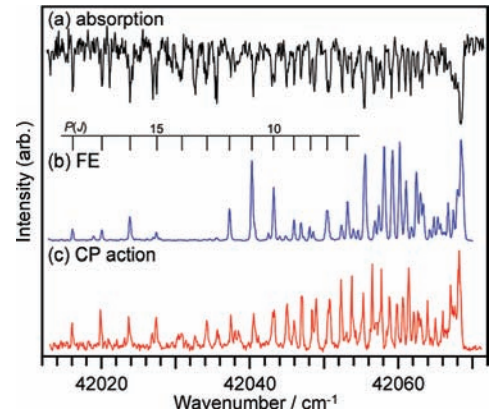

Figure 4. Expanded portion of the (a) absorption, (b) fluorescence excitation, and (c) CP action spectra of band 5 of HCP.

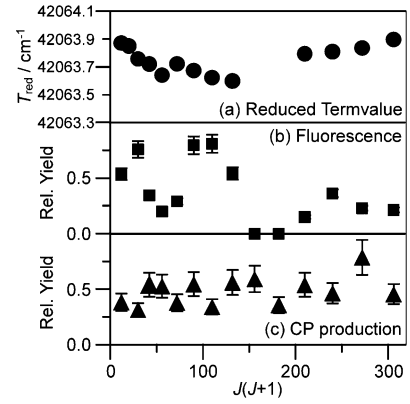

Figure 5. Plots of (a) reduced termvalue, (b) fluorescence, and (c) CP production yields against $J(J + 1)$. Typical uncertainties are indicated by bars in plots (b) and (c).

positions of the local perturbations indicated as discontinuities, the reduced termvalues, T_{red}, rather than total rovibronic termvalues, T, were plotted in the figure. The T_{red} is defined here as

$$T_{red} = T - \bar{B}J(J + 1) \quad (4)$$

where the value of $\bar{B}$ in the Figure 5 was set to 0.59 cm^{-1}. It is already known that there are many accidental or local rotational perturbations with the triplet states in the electronic states of singlet HCP.[24,41]

The relative fluorescence yield exhibits some irregular patterns, as indicated by the FE spectrum. At the very points of

these irregularities, discontinuities are found in the reduced term value plot. This indicates that the irregular fluorescence yield comes from the perturbation with the triplet states. In contrast, there is no $J(J+1)$ dependence in the CP radical production. As mentioned above, a transition from the initially excited state to the $\tilde{X}\ ^1\Sigma^+$ state must occur before the dissociation. Since the upper electronic state of band 5 is the $\tilde{A}\ ^1A''$ state, a Coriolis type coupling between the two electronic states is the most possible interaction. The matrix element for the Coriolis coupling around the *a*-axis is proportional to K_a, whereas it is $[J(J+1) - K_{b,c}^2]^{1/2}$ for the Coriolis coupling around the *b*- or *c*-axis. No $J(J+1)$ dependence of the CP production yield is consistent with the *a*-axis Coriolis coupling. Our results confirmed that the interaction between the $\tilde{A}$ and the $\tilde{X}$ states is the Coriolis coupling around the *a*-axis. The electronic configuration of the $\tilde{A}\ ^1A''$ state is a $\pi_{CP}\pi_{CP}^*$. The direction of the *a*-axis is closely parallel to the CP bond, and the rotation around the *a*-axis has a A'' symmetry. Thus, the predissociation mechanism due to the *a*-type Coriolis coupling is consistent with the symmetry consideration. Another perpendicular band (band 6) was examined in the same way, and the same lack of $J(J+1)$ dependence of the CP production yield was obtained.

We also examined parallel bands (bands 4 and 7) in the same manner. Trends are the same as those for the perpendicular band. The relative fluorescence yields exhibit some irregular patterns. At the points where the irregular pattern appears, the termvalue plot also indicates local perturbations.

In the case of the parallel band excitation, the relative CP production yields also exhibit no $J(J+1)$ dependence. The upper electronic state, $\tilde{C}\ ^1A'$, has the same symmetry as the $\tilde{X}$ state in the bent configuration. In this case, the nonadiabatic interaction between the $\tilde{X}$ and the $\tilde{C}$ states along the bending coordinate is the most probable interaction, which was suggested by Nanbu and co-workers.[34] In this case, no *J* dependence is expected, since the symmetry of the $\tilde{X}$ and the $\tilde{C}$ states is the same. This is also consistent with our consideration.

A relative yield between the fluorescence and the CP generation cannot be obtained in our observation. However, effects of the perturbation with the triplet state have appeared only in the fluorescence yield and not in the CP production yield. Thus, it is considered that the CP production is the major path, whereas the fluorescence is the minor one. The latter process sensitively reflects the effect of the perturbation by the triplet state.

3.4. Two Distinct Rotational Distributions of the CP Radical. Figure 6 shows a set of CP action spectra of HCP monitoring different rotational levels of the CP radical in the vicinity of the dissociation threshold. It is clearly seen that patterns of the spectra depend on the monitored rotational level of the CP radical. As mentioned in Section 3.2, only the rotational levels having a large enough energy to dissociate appear in the CP action spectra. If there would be no preference in rotational distribution of the CP radical, the action spectrum would become congested monotonically by lowering the rotational quantum number of CP radical monitored. For example, upper rotational levels excited by vibronic lines that appear in Figure 6a monitoring $N = 14$ have a large enough energy to produce smaller-*N* (<14) levels of CP. Thus, the lines that appear in Figure 6a should appear in Figure 6b−d. However, not all the strong lines in Figure 6a are absent in Figure 6b−d. This indicates that there is a rotational preference in the predissociation. Figure 7 shows LIF spectra of the CP radical produced from certain rotation−vibration levels of HCP. The pump transitions used are indicated by arrows in Figure 6.

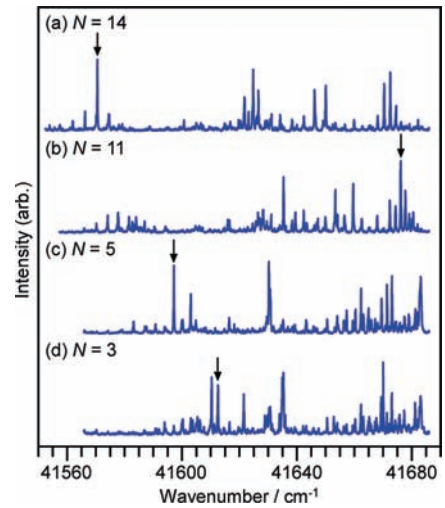

Figure 6. CP action spectra in the vicinity of the dissociation threshold monitoring different rotational levels of the CP radical. Rotational levels monitored are (a) 3, (b) 5, (c) 11, and (d) 14, respectively. Arrows indicate the rotational lines used as the pump transition for the measurement of the LIF spectra of the CP radical shown in Figure 7.

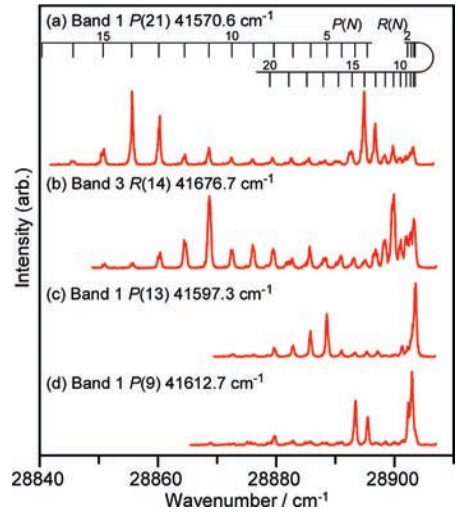

Figure 7. LIF spectra of the CP radical from a single rovibronic level of HCP. The pump transitions used are indicated in each trace, together with their wavenumbers and also in Figure 6 as arrows.

These spectra clearly exhibit nonstatistical rotational distribution of the CP radical.

Since a single rotational level is prepared as the initial state, values of the total energy and the angular momentum is precisely specified in our measurement. Some of rotational distributions of the product CP are displayed in Figure 8. In these cases, band 3 was used as the pump transition. Since the upper rotational levels of band 3 have a K_a value of 1, parity of each rotational level is specified by *e*- or *f*-symmetry. The rotational distributions originating from the *e*-symmetry components are shown in Figure 8a, whereas those from the *f*-symmetry components are shown in Figure 8b. In both cases, as the value of *J* increases, the peak of the rotational distribution shifts to higher *N*. In the case of the *e*-symmetry components, some of the distributions exhibit a very high preference to produce a high-*N* level.

To discuss the predissociation dynamics, rotational distributions obtained are compared with those expected by a statistical calculation based on the phase space theory (PST).[45] In the PST

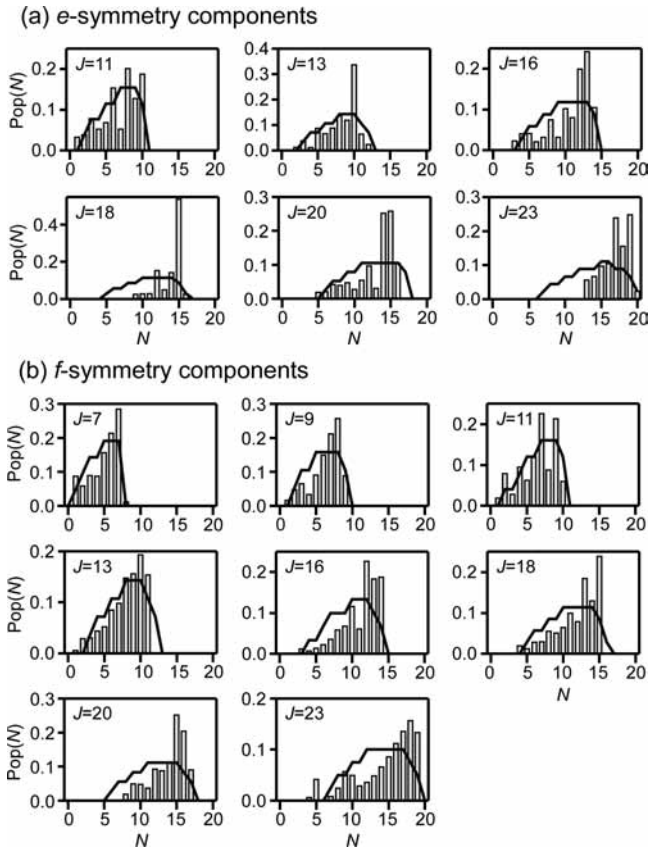

Figure 8. Rotational distributions of the CP radical produced single rovibronic levels of HCP. Band 3 is used as the pump transition. (a) *e*- and (b) *f*-Symmetry components are displayed separately. Populations of each rotational level are indicated as bars. Solid lines indicate the rotational distributions expected by the PST calculations.

calculation, it is assumed that all the final states that satisfy both the energy and the angular momentum conservation law are produced in the same probability. An impact parameter, which determines the recoil centrifugal barrier in the dissociation, is assumed to be 4 Å. The energy conservation condition is already shown in eq 1. The angular momentum conservation in this system is

$$\mathbf{J} = \mathbf{N} + \mathbf{S} + \mathbf{L} \tag{5}$$

where **J**, **N**, and **S** are angular momenta for the rotation of parent HCP, the rotation and spin of product CP radical, respectively. **L** is an orbital angular momentum of the recoil translation of the products. To make the following discussion simple, the effect of **S** is neglected here. The rotational distributions obtained by the PST calculation are also indicated in Figure 8. Comparing the observed rotational distributions with the calculated ones, it is found that higher-*N* levels are preferentially produced as compared to the PST expectation. In the larger *J* case, this trend, $\mathbf{N} \approx \mathbf{J}$, becomes obvious. In other words, the recoil orbital angular momentum **L** is very small in the dissociation of HCP.

When bands 4, 5, and 6 are used as the pump transition, distinct rotational distributions to those mentioned above are observed. Figure 9 exhibits this difference in the rotational distribution of the CP radical. In the case of band 4 excitation, the rotational distributions are well-reproduced by the PST calculation; that is, statistical distribution. In Figure 9, the rotational distributions obtained from the initial states having similar available energy are displayed in the same row to compare with each other. Although the difference in the available energy is very small, very distinct rotational distributions, nonstatistical and statistical, are obtained. The nonstatistical or preferential distribution observed in the cases of the excitation of bands 1−3 suddenly disappears with an increase in the vibronic energy. On the basis of this difference, the predissociation dynamics is discussed below.

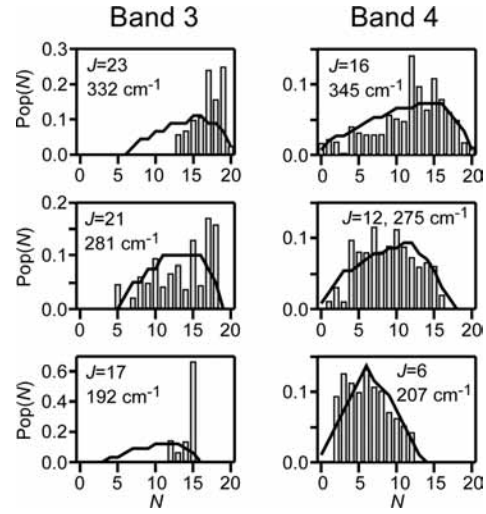

Figure 9. Comparison of the rotational distribution produced from the initial levels having a similar available energy. Rotational quantum number, *J*, and available energy in the dissociation of each case are indicated in the figure. Populations of each rotational level are indicated as bars. Solid lines indicate the rotational distributions expected by the PST calculations.

3.5. Predissociation Dynamics. Since the initially excited electronic state is not the same in the cases of bands 1−3, the above-mentioned preferential rotational distributions should not depend on the electronic state. Thus, the rotational distribution is considered to be determined by the dynamics in the $\tilde{X}$ state in the exit region to the dissociation. The main difference between the upper states of bands 1−3 and 4−6 is the composition of their energy. The vibronic energies of the upper levels in bands 1−3 are smaller than the D_0 (41 662.3 cm^{-1}) determined in the present study,[46] whereas those in bands 4−6 are larger than the D_0. That is, an intramolecular energy transfer from the rotational to the vibrational degrees of freedoms is necessary in the former case. Due to the energy and the angular momentum conservation, such an energy transfer should be accompanied by a large structural change in the dissociation.

Taking the above points into account, we consider the predissociation dynamics based on the potential energy surface of the $\tilde{X}$ state of HCP calculated by Nanbu and co-workers. They obtained a potential energy surface along the H−CP dissociation.[47] The minimum energy path to the dissociation to $H(^2S) + CP(X\,^2\Sigma^+)$ is along the linear H−C−P configuration near the dissociation limit. In addition, there is no substantial barrier in the region with large a H−CP distance. There is another experimental observation that is an important factor to discuss the dissociation dynamics. It is time constants of the dissociation. Figure 10 shows a typical time profile of the generation of the CP radical obtained by the pump−probe measurement. The risetime profile can be expressed as $C\,[1 - \exp(-t/\tau)]$, where *C* is a proportional constant and τ is a time constant of the CP radical generation. Convolving the time profiles of pump and probe laser pulses (3 ns each) with the rise profile, observed time profiles were simulated. In the case shown in Figure 10, the time constant was estimated to be 2.5 ns. The time constants of the dissociation are found to be 1−3 ns. This value is much longer than the rotational period and, thus, indicates that the dissociation is basically statistical.

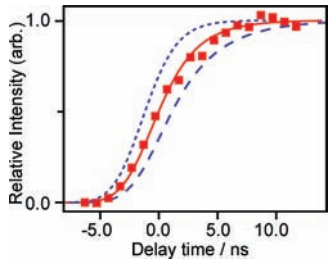

Figure 10. Temporal profile of the CP radical production against the delay time between the pump and the probe laser pulses. The pump transition is the $Q(7)$ line of band 3, and the probe transition is the P(7) line of the $B\,^2\Sigma^+ - X\,^2\Sigma^+$ (0−0) band of the CP radical. Filled squares indicate observed intensity. Simulated time profiles are indicated as dotted, solid, and broken lines with a time constant of 1.5, 2.5, and 3.5 ns, respectively. Simulated time profiles are obtained by convolving the laser pulse widths of 3 ns for the pump and probe pulses with the rise profile of the time constants indicated.

In the case of excitation in bands 4−6, the vibronic energy of the initial state, that is, the vibrational energy in the $\tilde{X}$state, is larger than the D_0. Since the bending potential is very shallow in the exit region of the potential energy surface, the excess vibrational energy enables bending excitation during the dissociation. This bending excitation should result in the statistical rotational distribution. On the other hand, in the case of excitation in bands 1−3, the vibronic energy is smaller than the D_0. As mentioned above, the intramolecular energy transfer from the rotational to the vibrational degrees of freedom is necessary for the dissociation. However, our result suggests that such an energy transfer seems not to occur efficiently and that the minimum amount of energy that is necessary for the dissociation is transferred. Thus, the dissociation should proceed along the minimum energy path that is along the linear H−C−P configuration. This geometric restriction in the dissociation along linear configuration results in the small value of **L** and preference of $\mathbf{N} \approx \mathbf{J}$. The two distinct rotational distributions can be qualitatively interpreted by the inefficient energy transfer from the rotational to the vibrational degrees of freedom in the exit region of the $\tilde{X}$ state potential energy surface. Our observation also suggests that the intramolecular energy transfer from the bending vibrational to the rotational degrees of freedom occurs efficiently in the cases except for the excitation in bands 1−3.

So far, we have investigated the predissociation dynamics of HCP in the very vicinity of the dissociation threshold. In the present study, we have also examined vibrational energy dependence on the rotational distribution of the CP radical. Here, we have excited HCP at the R-head of each vibronic band and have measured rotational distributions of the CP radical. The measured rotational distributions are similar to the statistical ones. Thus, assuming the Boltzman distribution, we have estimated the rotational temperature as the measure of the rotational excitation. Figure 11 shows the vibrational or excess energy dependence of the rotational distribution of the CP radical. A monotonic increase with the vibrational energy indicates statistical energy distribution. As shown in Figure 3, action spectra monitoring the different vibrational states of the CP radical are very similar to each other. This result also supports that the energy distribution is statistical in the higher energy region. The dissociation time constant of a few nanoseconds is consistent with the statistical energy distribution. These results indicate that the energy distribution in the predissociation of HCP is basically statistical.

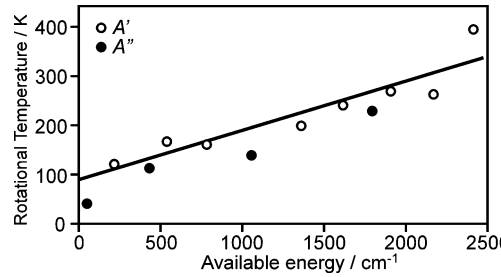

Figure 11. Available energy dependence of the rotational distribution of the CP radical. The rotational distributions are indicated by the rotational temperature. Open and filled circles denote the results of the CP radical produced from the A′ and the A″ states, respectively.

4. Conclusions

In the present study, we have observed absorption, FE, and CP radical action spectra of the HCP molecule in the vicinity of the dissociation threshold. It has been confirmed that the sudden decrease in the fluorescence intensity originally observed by Mason and Lehmann is due to predissociation to $H(^2S) + CP(X\,^2\Sigma^+)$. We have measured the rotational distribution of the CP radical generated by the systematic selection of the rotationally resolved excitation of the parent HCP molecule. The energetic consideration between the parent and product rovibronic energies has enabled us to determine the dissociation energy to be $41\,662.3 \pm 0.5$ cm^{-1}. On the basis of comparison among absorption, FE, and CP radical action spectra of the parent HCP molecule, it has been interpreted that the dissociation is the major process and the fluorescence decay is the minor one. The latter is perturbed by the interaction with the triplet state. The energy distribution in the predissociation of HCP is found to be basically statistical. However, the prominent preference in the rotational distribution is observed only when the vibronic energy is smaller than the D_0. The two distinct rotational distributions can be qualitatively interpreted by the inefficient energy transfer from the rotational to the vibrational degrees of freedom in the exit region of the $\tilde{X}$ state potential energy surface. Since the HCP molecule follows the minimum energy path to the dissociation, which is along the linear H−C−P configuration, the recoil orbital angular momentum, **L**, becomes small, and it results in the nonstatistical rotational distribution. Our study suggests that the energy transfer from the rotational to the vibrational degrees of freedom is inefficient, whereas the inverse process is efficient in the dissociation of HCP.

Acknowledgment. The authors are very grateful to Prof. Shinko Nanbu (Kyushu University) for a valuable discussion and providing us with some unpublished results. They also would like to thank Dr. Shigeru Sasaki (Tohoku University) for synthesis of the precursor $CHCl_2PH_2$ molecule.

References and Notes

(1) Ishikawa, H.; Field, R. W.; Farantos, S. C.; Joyeux, M.; Koput, J.; Beck, C.; Schinke, R. *Annu. Rev. Phys. Chem.* **1999**, *50*, 443.
(2) Lehmann, K. K.; Ross, S. C.; Lohr, L. L. *J. Chem. Phys.* **1985**, *82*, 4460.
(3) Chen, Y.-T.; Watt, D. M.; Field, R. W.; Lehmann, K. K. *J. Chem. Phys.* **1990**, *93*, 2149.
(4) Ishikawa, H.; Chen, Y.-T.; Ohshima, Y.; Wang, J.; Field, R. W. *J. Chem. Phys.* **1996**, *105*, 7383.
(5) Ishikawa, H.; Nagao, C.; Mikami, N.; Field, R. W. *J. Chem. Phys.* **1997**, *106*, 2980.
(6) Ishikawa, H.; Nagao, C.; Mikami, N.; Field, R. W. *J. Chem. Phys.* **1998**, *109*, 492.
(7) Ishikawa, H.; Nagao, C.; Mikami, N. *Chem. Lett.* **1999**, *28*, 941.

(8) Ishikawa, H.; Toyosaki, H.; Mikami, N.; Pérez-Bernal, F.; Vaccaro, P. H.; Iachello, F. *Chem. Phys. Lett.* **2002**, *365*, 57.
(9) Jung, M.; Winnewisser, B. P.; Winnewisser, M. *J. Mol. Struct.* **1997**, *413*, 31.
(10) Chen, Y.-T.; Chong, D. P. *J. Chem. Phys.* **1993**, *99*, 8870.
(11) Farantos, S. C.; Keller, H.-M.; Schinke, R.; Yamashita, K.; Morokuma, K. *J. Chem. Phys.* **1996**, *104*, 10055.
(12) Beck, C.; Keller, H. M.; Grebenshchikov, S. Y.; Schinke, R.; Farantos, S. C.; Yamashita, K.; Morokuma, K. *J. Chem. Phys.* **1997**, *107*, 9818.
(13) Grebenshchikov, S. Y.; Beck, C.; Schinke, R.; Farantos, S. C. *Phys. Lett.* **1998**, *243*, 208.
(14) Beck, C.; Schinke, R.; Koput, J. *J. Chem. Phys.* **2000**, *112*, 8446.
(15) Bredenbeck, J.; Beck, C.; Schinke, R.; Koput, J.; Stamatiadis, S.; Farantos, S. C.; Joyeux, M. *J. Chem. Phys.* **2000**, *112*, 8855.
(16) Koput, J. *Chem. Phys. Lett.* **1996**, *263*, 401.
(17) Koput, J.; Carter, S. *Spectrochim. Acta A* **1997**, *53*, 1091.
(18) Joyeux, M.; Sugny, D.; Tyan, V.; Kellman, M. E.; Ishikawa, H.; Field, R. W.; Beck, C.; Schinke, R. *J. Chem. Phys.* **2000**, *112*, 4162.
(19) Joyeux, M.; Farantos, S. C.; Schinke, R. *J. Phys. Chem. A* **2002**, *106*, 5407.
(20) Joyeux, M.; Sugny, D. *Can. J. Phys.* **2002**, *80*, 1459.
(21) Jacobson, M. P.; Child, M. S. *J. Chem. Phys.* **2001**, *114*, 250.
(22) Jacobson, M. P.; Child, M. S. *J. Chem. Phys.* **2001**, *114*, 262.
(23) Safi, Z. S.; Losada, J. C.; Benito, R. M.; Borondo, F. *J. Chem. Phys.* **2008**, *129*, 164316.
(24) Johns, J. W. C.; Shurvell, H. F.; Tyler, J. K. *Can. J. Phys.* **1969**, *47*, 893.
(25) Moehlmann, J. G.; Hartford, A.; Lombardi, J. R. *Can. J. Phys.* **1972**, *50*, 1705.
(26) Karna, S. P.; Bruna, P. J.; Grein, F. *Can. J. Phys.* **1990**, *68*, 499.
(27) Mason, M. A.; Lehmann, K. K. *J. Chem. Phys.* **1993**, *98*, 5184.
(28) Mason, M. A. Ph.D. Thesis, Department of Chemistry, Princeton University, Princeton, NJ, 1995.
(29) Sasaki, T.; Ishikawa, H.; Nagao, C.; Mikami, N. (unpublished), 1997.
(30) Chen, Y.-T.; Wang, J.; Coy, S. L.; Field, R. W. (unpublished), 1991.
(31) Rajaram, B. Ph.D. Thesis, Department of Chemistry, Massachusetts Institute of Technology, Cambridge, MA, 1995.
(32) Sannigrahi, A. B.; Grein, F. *Chem. Phys. Lett.* **1993**, *214*, 609.
(33) Goldstein, E.; Jin, S.; Carrillo, M. R.; Cave, R. J. *J. Comput. Chem.* **1993**, *14*, 186.
(34) Nanbu, S.; Gray, S. K.; Kinoshita, T.; Aoyagi, M. *J. Chem. Phys.* **2000**, *112*, 5866.
(35) Ingels, J. B.; Turney, J. M.; Richardson, N. A.; Yamaguchi, Y.; Schaefer, H. F., III *J. Chem. Phys.* **2006**, *125*, 104306.
(36) Houston, P. L. *J. Phys. Chem.* **1987**, *91*, 5388.
(37) Schinke, R. *Annu. Rev. Phys. Chem.* **1988**, *39*, 39.
(38) Hall, G. E.; Houston, P. L. *Annu. Rev. Phys. Chem.* **1989**, *40*, 375.
(39) Schinke, R. *Photodissociation Dynamics*; Cambridge University Press: Cambridge, 1993.
(40) Gordon, R. J.; Hall, G. E. *Adv. Chem. Phys.* **1996**, *116*, 1.
(41) Ishikawa, H.; Nagao, C.; Mikami, N. *J. Mol. Spectrosc.* **1999**, *194*, 52.
(42) Cariou, J.; Luc, P. *Atlas du Spectre d'Absorption de la Molécule de Tellure*; CNRS: Paris, 1980.
(43) Bärwald, V. H.; Herzberg, G.; Herzberg, L. *Ann. Phys.* **1934**, *20*, 569.
(44) As described in Section 3.4, there is a preference in rotational distribution of small **L** in the cases of the dissociation at bands 1−3. Thus, the neglect of the centrifugal barrier is considered to be acceptable.
(45) Pechukas, P.; Light, J. C.; Rankin, C. *J. Chem. Phys.* **1966**, *44*, 794.
(46) The ν_0 value of band 3 listed in Table 1 is larger than the D_0. However, it contains the A rotational constant. Thus, the vibronic energy of the upper level of band 3 is considered to be smaller than the D_0.
(47) Nanbu, S. Private communication.

JP900450T